DE GRUYTER Main Group Met. Chem. 2019; 42: 135–142

Research Article **Open Access**

Mehmet Fatih Kaya, Özgür Alver, Cemal Parlak and Ponnadurai Ramasami*

Theoretical insight of alpha amino acid phenylalanine adsorption on pristine and decorated fullerenes

https://doi.org/10.1515/mgmc-2019-0015
Received February 25, 2019; accepted May 10, 2019.

Abstract: Fullerenes, with their extensive application potentials, have been receiving attention for their possible usage as drug delivery vehicles and devices for sensor technologies. In this work, the optimized molecular geometries, some diagnostic geometric parameters, electronic characteristics, natural bond orbital examinations and the interaction phenomena between C_{60}, Si- or Al-doped C_{60} and phenylalanine amino acid molecule were investigated by the quantum mechanical calculations. It is observed that the impurity addition and using water as the solvent intensify the interaction between fullerene and amino acid system. These lead to various alterations in the electronic properties and NH stretching values of the clusters studied.

Keywords: adsorption; fullerenes; amino acids; phenylalanine; DFT

1 Introduction

Fullerenes also known as buckminsterfullerenes are classes of soccer ball-shaped carbon molecules; discovered in 1985 (Kroto et al., 1985). The most representative member of the fullerene family is composed of 60 carbon atoms arranged in a spherical structure. There are two types of bonds in the fullerene: 60 C–C single bonds in the pentagons and 30 C=C double bonds in the hexagons. Fullerenes are exceptional free radical scavengers (Krusic et al., 1991). They can entrap free radicals and neutralize them before they lead any cellular disorder. Because of this unique physicochemical properties, recently there has been much interest in searching for possible biological activities of fullerenes with a view to use them in area of medicine such as anti-cancer and anti-bacterial agents (Kai et al., 2003; Poland et al., 2008; Triesscheijn et al., 2006), photodynamic therapy (Mroz et al., 2007; Sharma and Chiang, 2011), enzyme inhibition (Abellán-Flos et al., 2015; Innocenti et al., 2010), antiviral activity (Ji et al., 2008; Medzhidova et al., 2003), DNA cleavage (Kumar et al., 2009) and electron transfer (Kuciauskas et al., 1996; Wróbel and Graja, 2011). An important problem to be solved with undecorated fullerenes is their insolubility in biologically compatible solvents thus hindering their possible applications. Henceforth, chemical modification or functionalization of fullerenes with different types of addends such as impurity atoms appear as an option to intensify their solubilities (Brettreich and Hirsch, 1998; Da Ros et al., 1996; Foley et al., 2002). The water-soluble fullerenes have been proved to reduce the level of intracellular peroxidation (Xiao et al., 2005).

Phenylalanine (Phe) is an α-amino acid with the formula $C_6H_5CH_2CH(NH_2)COOH$. Genetic disorder phenyl ketenuria (PKU) is a result of metabolism problems of phenylalanine (Tachibana et al., 2006). High level of phenylalanine accumulation in blood leads to damage especially in brain development (De Groot et al., 2010; van Spronsen and Enns, 2010). Untreated PKU causes some mental and so the social problems in following ages (Demirkol et al., 2011; Rocha and Martel, 2009).

*** Corresponding author: Ponnadurai Ramasami,** Computational Chemistry Group, Department of Chemistry, Faculty of Science, University of Mauritius, Réduit 80837, Mauritius; Department of Applied Chemistry, University of Johannesburg, Doornfontein Campus, Johannesburg 2028, South Africa, e-mail: p.ramasami@uom.ac.mu, Tel: +230 4037507
Mehmet Fatih Kaya, Department of Physics, Faculty of Sciences and Arts, Piri Reis University, Istanbul, Turkey
Özgür Alver, Department of Physics, Science Faculty, Eskisehir Technical University, 26470, Turkey
Cemal Parlak, Department of Physics, Science Faculty, Ege University, Izmir, 35100, Turkey

Density functional theory (DFT) is a computational method which is widely used for identification and pre-evaluation of different types of compounds and molecular systems (Alver and Parlak, 2010; Bouabdallah et al., 2016; Jadoo et al., 2018). DFT is considered as an alternative for the solution of many-electron problems instead of wave function methods. It is an exact theory but in practice the approximation of exchange-correlation energy is required (Sun et al., 2019).

In continuation with our interests in the investigation of interaction between drug and fullerene systems (Parlak and Alver, 2017; Parlak et al., 2017), we aimed to study the interactions of Phe with undoped and Si- or Al-doped C_{60} fullerenes using DFT methods in both gas phase and water. Despite some experimental difficulties, silicon and aluminium atoms have been successfully doped into fullerenes as reported in the previous works (Bashiri et al., 2017; Fu et al., 2015; Kimura et al., 1996). This fact was the main reason of the choice of silicon and aluminium atoms as dopants. The main motivation of this study is the possibility of using the results obtained to enlighten drug designs for the treatment of PKU.

2 Computational studies

The important part is the optimization of the complexes studied until no imaginary frequencies were obtained to make sure that the resultant structures belong to minima rather than a transition state. For this purpose, taking into account the possible active sites of Phe, several structures were built and optimized with the M062X and B3LYP functionals with the 6-31G(d) basis set in both the gas phase and water media. Electronic properties and stability assessments of the optimized structures were examined by calculating the binding energy (E_b), frontier molecular energy gap (E_g), chemical hardness (η) and electrophilicity indexes (ω).

In order to consider the effect of solvent on the stabilities and electronic properties, all the calculations were done in water. Natural bond orbital (NBO) analysis was also used to have a comprehensible perception of the charge distributions (Reed et al., 1985). Multiwfn program was also used to have more insights in the nature of bonding at interaction sides such as, Wiberg bond index (WBI) and Fuzzy bond order (FBO) (Lu and Chen, 2012). Gaussian, GaussView and GaussSum programs were used for the calculations and visualizations (Dennington et al., 2009; Frisch et al., 2009; O'Boyle et al., 2008).

3 Results and discussion

3.1 Analysis of C_{60}...Phe interaction

Gas phase optimized structures for C_{60}...Phe are given in Figure 1. It is observed that the plane indicated by

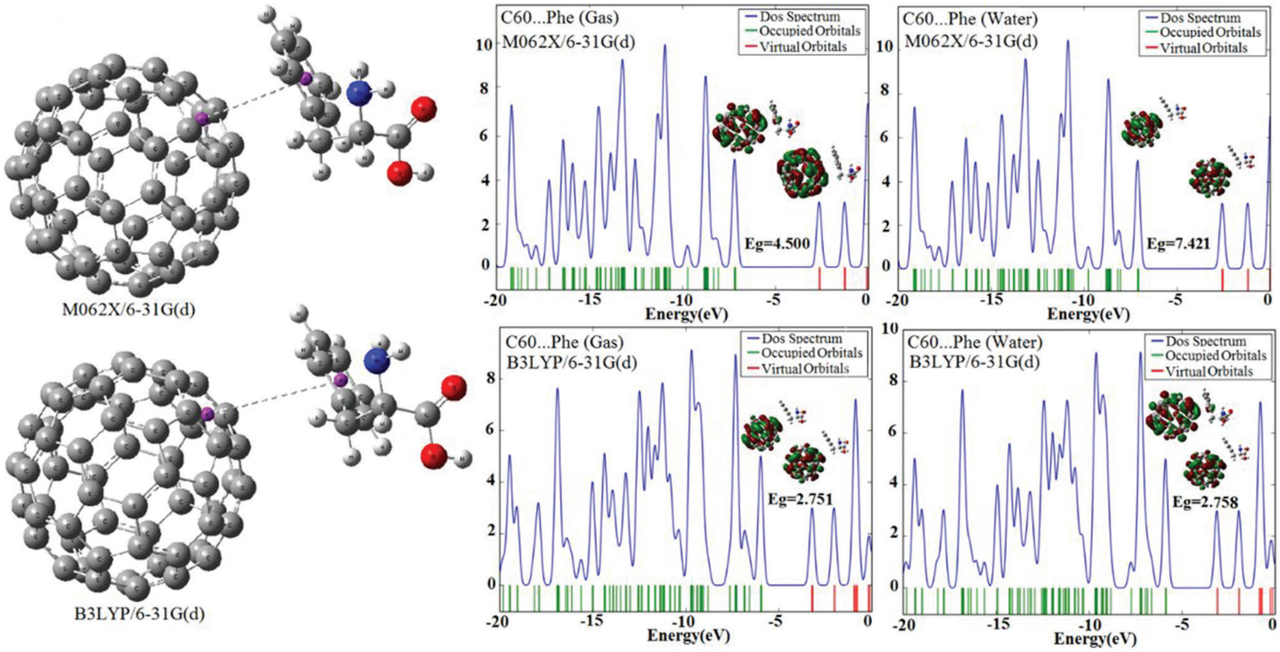

Figure 1: The optimized structures and DOS spectrum of C_{60}...Phe system.

hexagons of C_{60} orients almost parallel to the plane of the ring atoms of the Phe molecule. This leads to a parallel displaced π-π interactions which is more clearly described with M062X functional compared to B3LYP (Zhao and Truhlar, 2007). The E_b energies of C_{60}...Phe in the gas phase and water were found as -0.28 and -0.21 kcal/mol with the B3LYP, -5.97 and -5.24 kcal/mol with the M062X functional. These suggest that the nature of interaction between undoped C_{60} and Phe molecule occurs due to physisadsorption since E_b energies are less than 10 kcal/mol (Ameta and Penoni, 2014). The DOS graphs of C_{60}...Phe structure are also shown in Figure 1. It is observed that for calculations in water, the B3LYP functional yields a slight change (0.007 eV) in the gap energies compared to the gas phase calculations. However, results from the M062X functional yields a change about 2.92 eV. This difference in the gap energy arises from the fact that unlike B3LYP functional M062X overestimates E_g values (Soto-Rojo et al., 2014).

In order to measure the nearest rings of C_{60} and the drug molecule, dummy atoms were inserted at the centers of the rings as illustrated in Figure 1. This distance is predicated using the functional M062X in the gas phase and water as 3.61 Å and 3.60 Å, respectively. When the B3LYP functional was used, this distance was estimated as 4.38 Å and 4.45 Å in the gas phase and water.

3.2 Analysis of Al- and Si-doped systems

In order to identify possible interaction sites for a given molecular complex, careful examinations and identification of charge distribution along the molecular surfaces of the structure investigated were carried out for the interaction edges (Armaković et al., 2014; Shariatinia and Shahidi, 2014). Analysis of charge distribution turns out to be an important process for the determination of possible adsorption sites. Charge distributions over the surface of the molecular structures determine the possible interaction sites on a given molecular system and they show dependence on types of the atoms in the structure and computational methods (Kelly et al., 2005; Suliman et al., 2014). Molecular electrostatic potential (MEP) maps allow to analyse the charge distributions of molecular systems in three dimension.

On the basis of the possible interaction edges based on charge distribution analysis (see Figure S1 in Supplementary material) of Phe, four different interaction sites were proposed between the Phe and doped C_{60} fullerenes (Figure 2). These interaction edges were labelled as C=O&NH_2, NH_2, C=O, C=O&OH. In the given configurations, aluminum and silicon atoms were considered as the active sites (Parlak and Alver, 2017; Parlak et al., 2017). E_b was calculated out for AlC_{59}...Phe and SiC_{59}...Phe systems in both the gas phase and water. The results indicate that AlC_{59}...Phe (NH_2) and SiC_{59}...Phe (NH_2) complexes have the highest E_b energies in magnitude in both the gas phase and water (Table 1). Thus Phe molecule is most likely to be adsorbed from NH_2 site and this is more effective compared to C=O&NH_2, C=O and C=O&OH interaction edges. The E_b values for the Al- and Si-doped fullerenes suggest that the strength of the interaction is in the range of chemisorption as a value of larger than 10 kcal/mol is an indicator of a possible chemisorption (Ameta and Penoni, 2014). The solvent energies (E_s) are given in Table 1 and these imply that AlC_{59}...Phe (NH_2) and SiC_{59}...Phe (NH_2) complexes are likely to be soluble in water with values of -18.77 (B3LYP), -19.25 (M062X) and -19.45 (B3LYP), -20.60 kcal/mol (M062X), respectively.

The values of chemical hardness and electrophilicity indexes, chemical stability and reactivity of chemical species can be evaluated (Oura et al., 2003). Chemical hardness values of Al-doped fullerene complexes are larger in water compared to gas phase with both functionals. For Si-doped complexes, the values of chemical hardness are found to be dependent on the interaction site and the choice of basis sets. In fact, while the results with B3LYP functional indicate slight decrease for SiC_{59}...C=O&NH_2 and SiC_{59}...NH_2, slight increase was observed for SiC_{59}...C=O and SiC_{59}...C=O&OH complexes in the chemical hardness values. It was also observed that electrophilicity indexes appeared strongly dependent on the interaction sites of the complexes investigated. From Table 2, the band gap energies for Al-doped fullerenes are larger for water than in the gas phase. The band gap energy values of the Si-doped complexes show dependence on interaction site of the ligand molecule.

It is known in chemisorption, new chemical bonds between interacting molecules are formed and thus the interatomic distances where the possible bonds are formed must be at proper length (El Mahdy, 2016). Some relevant internuclear distances are given in Table 3. It is observed that related internuclear distances generally tend to decrease in water to make more stable complexes and the distances calculated are in the range possible for chemisorption (Table 2) (De Silva et al., 2014; Hassani and Tavakol, 2014). In order to support possible chemisorption sites, MEP diagram was calculated with M062X functional with the 6-31G(d) basis set for AlC_{59}...NH_2 complex in the gas phase as illustrated in

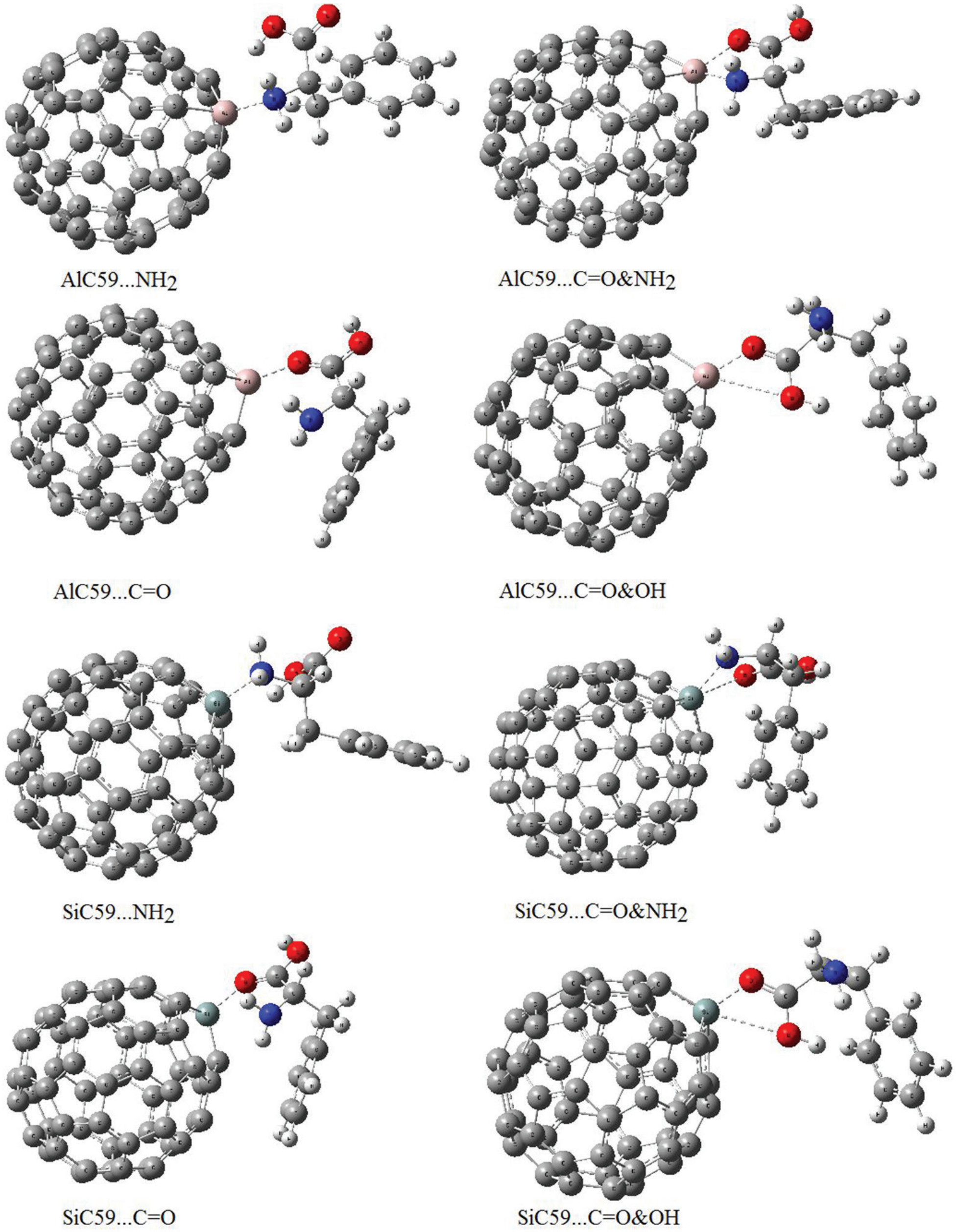

AlC59...NH2

AlC59...C=O&NH2

AlC59...C=O

AlC59...C=O&OH

SiC59...NH2

SiC59...C=O&NH2

SiC59...C=O

SiC59...C=O&OH

Figure 2: Possible interaction edges and optimized structures for the doped systems with B3LYP/6-31G(d).

Table 1: Binding and solvent energies (kcal/mol) of the investigated systems.

Structure	M062X/6-31G(d)			B3LYP/6-31G(d)		
	E_b(gas)	E_b(water)	E_s	E_b(gas)	E_b(water)	E_s
C_{60}...Phe	-5.97	-5.24	-6.71	-0.28	-0.21	-7.11
AlC_{59}...C=O&NH_2	-46.90	-47.63	-12.03	-32.19	-39.27	-17.26
AlC_{59}...NH_2	-52.15	-60.09	-19.25	-40.90	-49.48	-18.77
AlC_{59}...C=O	-50.37	-52.39	-13.32	-37.15	-39.64	-12.68
AlC_{59}...C=O&OH	-40.02	-43.52	-14.81	-34.16	-38.71	-14.74
SiC_{59}... C=O&NH_2	-29.49	-39.29	-17.76	-16.75	-26.28	-16.82
SiC_{59}...NH_2	-36.07	-48.70	-20.60	-17.56	-29.71	-19.45
SiC_{59}...C=O	-32.35	-38.97	-14.59	-15.36	-22.57	-14.50
SiC_{59}...C=O&OH	-24.52	-33.48	-16.92	-14.01	-23.46	-16.75

Table 2: Some energetic parameters (eV) of the investigated systems.

Structure	B3LYP/6-31G(d)				
	HOMO	LUMO	Gap	Chemical hardness	Electrophilicity index
			Gas		
C_{60}...Phe	-5.942	-3.191	2.751	1.375	2.283
AlC_{59}... C=O&NH_2	-4.497	-3.013	1.484	0.742	1.877
AlC_{59}...NH_2	-5.095	-3.609	1.486	0.743	2.176
AlC_{59}...C=O	-4.739	-3.238	1.502	0.751	1.994
AlC_{59}...C=O&OH	-4.526	-3.012	1.514	0.757	1.884
SiC_{59}...C=O&NH_2	-4.567	-2.464	2.103	1.052	1.758
SiC_{59}...NH_2	-5.013	-2.915	2.098	1.049	1.982
SiC_{59}...C=O	-4.691	-2.846	1.844	0.922	1.884
SiC_{59}...C=O&OH	-4.442	-2.781	1.661	0.831	1.806
			Water		
C_{60}...Phe	-5.865	-3.107	2.758	1.379	2.243
AlC_{59}... C=O&NH_2	-4.714	-3.190	1.523	0.762	1.976
AlC_{59}...NH_2	-5.035	-3.516	1.519	0.760	2.138
AlC_{59}...C=O	-4.933	-3.411	1.522	0.761	2.086
AlC_{59}...C=O&OH	-4.888	-3.357	1.531	0.765	2.061
SiC_{59}...C=O&NH_2	-4.714	-2.760	1.955	0.977	1.868
SiC_{59}...NH_2	-4.939	-2.922	2.017	1.009	1.965
SiC_{59}...C=O	-4.838	-2.831	2.007	1.004	1.917
SiC_{59}...C=O&OH	-4.767	-2.796	1.971	0.985	1.891
			M062X/6-31G(d) Gas		
C_{60}...Phe	-7.138	-2.638	4.500	2.250	2.444
AlC_{59}... C=O&NH_2	-5.600	-2.548	3.052	1.526	2.037
AlC_{59}...NH_2	-5.878	-2.819	3.059	1.530	2.174
AlC_{59}...C=O	-5.816	-2.675	3.141	1.571	2.123
AlC_{59}...C=O&OH	-5.632	-2.539	3.093	1.547	2.043
SiC_{59}...C=O&NH_2	-5.628	-1.911	3.717	1.858	1.885
SiC_{59}...NH_2	-6.125	-2.374	3.750	1.875	2.125
SiC_{59}...C=O	-5.766	-2.075	3.691	1.846	1.960
SiC_{59}...C=O&OH	-5.569	-1.884	3.685	1.842	1.863
			Water		
C_{60}...Phe	-7.536	-0.115	7.421	3.711	1.913
AlC_{59}... C=O&NH_2	-5.799	-2.686	3.113	1.556	2.121
AlC_{59}...NH_2	-6.133	-3.021	3.112	1.556	2.289
AlC_{59}...C=O	-5.992	-2.810	3.182	1.591	2.200
AlC_{59}...C=O&OH	-5.981	-2.858	3.123	1.561	2.210
SiC_{59}...C=O&NH_2	-5.781	-2.233	3.548	1.774	2.004
SiC_{59}...NH_2	-6.055	-2.408	3.647	1.824	2.116
SiC_{59}...C=O	-5.888	-2.312	3.575	1.788	2.050
SiC_{59}...C=O&OH	-5.880	-2.296	3.584	1.792	2.044

Figure 3. Overlapping high electron density between the NH_2 edge of Phe and the aluminium atom of fullerene cage can be seen in Figure 3 and this suggests possible bond formation due to chemisorption.

The NH_2 stretching vibrations are easy to identify and they show characteristic band properties. Since AlC_{59}...NH_2 and SiC_{59}...NH_2 complexes have the largest E_b energy, we examined the vibrational frequency alterations upon interaction of AlC_{59} and SiC_{59} with Phe molecule. The results obtained were from the M062X/6-31G(d) method. NH_2 antisymmetric and symmetric stretching vibrations changes by about 35, 48 cm^{-1} (gas phase) and 82, 57 cm^{-1} (water phase) for AlC_{59}...NH_2. As, these values were found as 98, 88 cm^{-1} (gas phase) and 106, 80 cm^{-1} (water phase)

Table 3: Internuclear distances of the investigated systems.

Interatomic distances (Å)*	M062X/6-31G(d)		B3LYP/6-31G(d)	
	Gas	Water	Gas	Water
AlC$_{59}$...C=O&**N**H$_2$	2.21	2.08	2.23	2.10
AlC$_{59}$...C=**O**&NH$_2$	2.01	2.01	2.07	2.05
AlC$_{59}$...**NH**$_2$	2.01	1.99	2.04	2.01
AlC$_{59}$...C=**O**	1.89	1.85	1.91	1.87
AlC$_{59}$...C=**O**&OH	1.90	1.86	1.92	1.88
AlC$_{59}$...C=O&**O**H	2.90	2.95	3.12	3.10
SiC$_{59}$... C=O&**N**H$_2$	1.97	1.92	2.02	1.95
SiC$_{59}$... C=**O**&NH$_2$	3.01	2.90	3.16	2.98
SiC$_{59}$...**NH**$_2$	1.93	1.90	1.97	1.93
SiC$_{59}$...C=**O**	1.84	1.78	1.87	1.80
SiC$_{59}$...C=**O**&OH	1.85	1.79	1.87	1.80
SiC$_{59}$...C=O&**O**H	2.86	2.89	3.02	3.00

* Distances are measured from the atom indicated with bold letter.

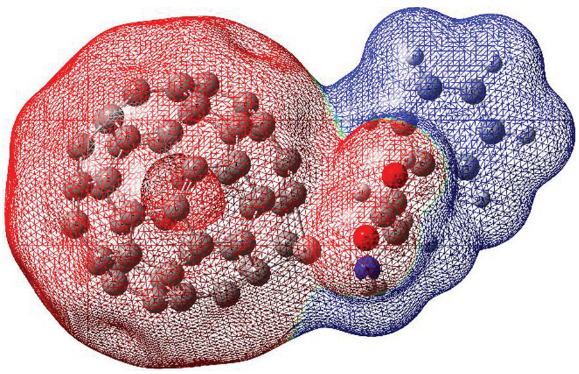

Figure 3: MEP on AlC$_{59}$...Phe (NH$_2$) system in gas phase. Color ranges, in a.u.: blue: more positive than 0.003 and red: more negative than -0.003.

for SiC$_{59}$...NH$_2$ complex. These changes in wavenumbers confirm the existence of interaction between the Phe and the doped fullerene system.

3.3 Population analysis

In order to make an analysis of interaction edges of Phe on fullerene nanocages, NBO theory was applied. NBO calculations provide useful information about molecular properties such as atomic charges and interaction between host and guest molecules or acceptor-donor pairs (Mahdavifar and Poulad, 2014). The calculated Mulliken and NBO charges address the formation of acceptor and donor pairs between Si/Al and N atoms in the complexes investigated (Table 4). The NBO analysis indicates that silicon atoms acquire positive charges or they become more positive following interaction between the doped fullerene cage and the Phe. This fact implies that the charge moves from the silicon atom to the nearby carbon atoms. As a result, silicon atom behaves as an affinity center for the possible chemisorption of Phe molecule. In the assessment of covalent bond character, like bond order values, WBI and FBO play important roles (Du et al., 2016). In this work, WBI indexes and FBO values were calculated as 0.65, 0.68 and 0.82, 0.93 for Al-N and Si-N bonds respectively, indicating the covalent bond character. From Table 4, it is also observed that valences of Al and Si atoms slightly increase because of the interaction with nitrogen atom of Phe.

Table 4: Population analysis of the selected systems.

Structure	Atom	Valence numbers	Mulliken charges	NBO charges
AlC$_{59}$	Al	3.324	0.392	1.650
SiC$_{59}$	Si	3.683	0.342	1.343
Phe	N	2.540	-0.699	-0.889
AlC$_{59}$...NH$_2$	Al	3.546	0.416	1.708
	N	2.912	-0.798	-0.976
SiC$_{59}$...NH$_2$	Si	4.044	0.597	1.928
	N	2.912	-0.789	-0.954

4 Conclusions

The physical interactions between the Si-, Al-doped and undoped C$_{60}$ fullerenes were examined based on the quantum mechanical calculations by DFT with M062X/6-31G(d) and B3LYP/6-31G(d) methods in the gas phase and water. Four possible interaction sites were proposed for the title molecule based on the molecular electrostatic surfaces analysis and their stabilities addressed dependence on the medium. It was observed that Al- and Si-doped systems increase in stability and show more negative binding energies in water compared to the gas phase. Furthermore, AlC$_{59}$...NH$_2$ and SiC$_{59}$...NH$_2$ systems result with the largest E$_b$ energies in magnitude with -52.15, -60.09 kcal/mol (gas phase and water with M062X) and -40.90, -49.48 kcal/mol (gas phase and water with B3LYP). Band gap energies of Al-doped fullerene structure were found smaller than the Si-doped structure. NBO calculations along with partial charge examinations and the calculated values of WBI and FBO address a possible bonding between Al/Si atoms of the doped fullerene cages and nitrogen atom of Phe molecule.

Acknowledgment: This work was supported by the Scientific Research Projects Commission of Eskisehir Technical University (Project No: 1606F564).

References

Abellán-Flos M., Tanç M., Supuran C.T., Vincent S.P., Exploring carbonic anhydrase inhibition with multimeric coumarins displayed on a fullerene scaffold. Org. Biomol. Chem., 2015, 13, 7445-7451.

Alver Ö., Parlak C., DFT, FT-Raman, FT-IR, liquid and solid state NMR studies of 2,6-dimethoxyphenylboronic acid. Vib. Spect., 2010, 54, 1-9.

Ameta K.L., Penoni A., Heterogeneous catalysis: A versatile tool for the synthesis of bioactive heterocycles. CRC press, 2014.

Armaković S., Armaković S.J., Šetrajčić J.P., Jaćimovski S.K., Holodkov V., Sumanene and its adsorption properties towards CO, CO_2 and NH_3 molecules. J. Mol. Model., 2014, 20, 2170.

Bashiri S., Vessally E., Bekhradnia A., Hosseinian A., Edjlali L., Utility of extrinsic [60] fullerenes as work function type sensors for amphetamine drug detection: DFT studies. Vacuum, 2017, 136, 156-162.

Bouabdallah S., Ben Dhia M.T., Driss M.R., Touil S., Investigation of the energy barrier to the rotation of amide CN bonds in ACE inhibitors by NMR, dynamic HPLC and DFT. J. Pharm. Biomed. Anal., 2016, 128, 416-425.

Brettreich M., Hirsch A., A highly water-soluble dendro[60]fullerene. Tetrahedron Lett., 1998, 39, 2731-2734.

Da Ros T., Prato M., Novello F., Maggini M., Banfi E., Easy access to water-soluble fullerene derivatives via 1,3-dipolar cycloadditions of azomethine ylides to C_{60}. J. Org. Chem., 1996, 61, 9070-9072.

De Groot M.J., Hoeksma M., Blau N., Reijngoud D.J., van Spronsen F.J., Pathogenesis of cognitive dysfunction in phenylketonuria: Review of hypotheses. Mol. Genet. Metab., 2010, 99, 86-89.

Demirkol M., Giżewska M., Giovannini M., Walter J., Follow up of phenylketonuria patients. Mol. Genet. Metab., 2011, 104, 31-39.

Dennington R., Keith T., Millam J., Semichem Inc. Shawnee Mission, KS, 2009.

De Silva S.W., Du A., Senadeera W., Gu Y., Neutral and charged boron-doped fullerenes for CO_2 adsorption. Beilstein J. Nanotechnol., 2014, 5, 413-418.

Du J., Sun X., Zhang C., The hydrogen storage on heptacoordinate carbon motif CTi_7^{2+}. Int. J. Hydrogen Energ., 2016, 41, 11301-11307.

El Mahdy A.M., Density functional investigation of CO and NO adsorption on TM-decorated C_{60} fullerene. Appl. Surf. Sci., 2016, 383, 353.

Foley S., Crowley C., Smaihi, M., Bonfils C., Erlanger B.F., Seta P., et al., Cellular localisation of a water-soluble fullerene derivative. Biochem. Biophys. Res. Commun., 2002, 294, 116-119.

Frisch M.J., Trucks G.W., Schlegel H.B., Scuseria G.E., Robb M.A., Cheeseman J.R., et al., Gaussian 09, Revision A.1. Gaussian Inc., Wallingford, CT, 2009.

Fu X., Wang Q.D., Liu Z., Peng F., Si-doped carbon nanotubes as efficient metal-free electrocatalysts for O_2 reduction in alkaline medium. Mater. Lett., 2015, 158, 32-35.

Hassani F., Tavakol H., A DFT, AIM and NBO study of adsorption and chemical sensing ofiodine by S-doped fullerenes. Sens. Actuators B, 2014, 196, 624-630.

Innocenti A., Durdagi S., Doostdar N., Strom T.A., Barron A.R., Supuran C.T., Nanoscale enzyme inhibitors: Fullerenes inhibit carbonic anhydrase by occluding the active site entrance. Bioorg. Med. Chem., 2010, 18, 2822-2828.

Jadoo B., Booysen I.N., Akerman M.P., Rhyman L., Ramasami P., Novel coumarin rhenium(I) and -(V) complexes: Formation, DFT and DNA binding studies. Polyhedron, 2018, 144, 107-118.

Ji H., Yang Z., Jiang W., Geng C., Gong M., Xiao H., et al., Antiviral activity of nano carbon fullerene lipidosome against influenza virus in vitro. J. Huazhong. Univ. Sci. Technol. Med. Sci., 2008, 28, 243-246.

Kai Y., Komazawa Y., Miyajima A., Miyata N., Yamakoshi Y., Fullerene as a novel photoinduced antibiotic. Fuller. Nanotub. Car. N., 2003, 11, 79-87.

Kelly C.P., Cramer C.J., Truhlar D.G., Accurate partial atomic charges for high-energy molecules using class IV charge models with the MIDI! basis set. Theor. Chem. Acc., 2005, 113, 133-151.

Kimura T., Sugai T., Shinohara H., Production and characterization of boron- and silicon-doped carbon clusters. Chem. Phys. Lett., 1996, 256, 269-273.

Kroto H.W., Heath J.R., Obrien S.C., Curl R.F., Smalley R.E., C_{60}: Buckminsterfullerene. Nature, 1985, 318, 162-163.

Krusic P.J., Wasserman E., Keizer P.N., Morton J.R., Preston K.F., Radical reactions of C_{60}. Science, 1991, 254, 1183-1185.

Kuciauskas D., Lin S., Seely G.R., Moore A.L., Moore T.A., Gust D., et al., Energy and photoinduced electron transfer in porphyrin–fullerene dyads. J. Phys. Chem., 1996, 100, 15926-15932.

Kumar A., Rao M.V., Menon S.K., Photoinduced DNA cleavage by fullerene–lysine conjugate. Tetrahedron Lett., 2009, 50, 6526-6530.

Lu T., Chen F., Multiwfn: a multifunctional wavefunction analyzer. J. Comput. Chem., 2012, 33, 580-592.

Mahdavifar Z., Poulad M., Theoretical prediction of ozone sensing using pristine and endohedral metalloboron B_{80} fullerenes. Sensor Actuat. B Chem., 2014, 205, 26-38.

Medzhidova M.G., Abdullaeva M.V., Fedorova N.E., Romanova V.S., Kushch A.A., In vitro antiviral activity of fullerene amino acid derivatives in cytomegalovirus infection. Antibiot. Khimioter., 2003, 49, 13-20.

Mroz P., Pawlak A., Satti M., Lee H., Wharton T., Gali H., et al., Functionalized fullerenes mediate photodynamic killing of cancer cells: Type I versus Type II photochemical mechanism. Free Radic. Biol. Med., 2007, 43, 711-719.

O'Boyle N.M., Tenderholt A.L., Langner K.M., cclib: A library for package-independent computational chemistry algorithms. J. Comput. Chem., 2008, 29, 839-845.

Oura K., Lifshits V.G., Saranin A., Zotov A.V., Katayama M., Surface Science, An Introduction. Springer, Berlin, 2003.

Parlak C., Alver Ö., Şenyel M., Computational study on favipiravir adsorption onto undoped and Si-doped C_{60} fullerenes. J. Theor. Comput. Chem., 2017, 16, 1750011.

Parlak C., Alver Ö., A density functional theory investigation on amantadine drug interaction with pristine and B, Al, Si, Ga, Ge doped C_{60} fullerenes. Chem. Phys. Lett., 2017, 678, 85-90.

Poland C.A., Duffin R., Kinloch I., Maynard A., Wallace W.A., Seaton A., et al., Carbon nanotubes introduced into the abdominal cavity of mice show asbestos-like pathogenicity in a pilot study. Nat. Nanotechnol., 2008, 3, 423-428.

Reed A.E., Weinstock R.B., Weinhold F., Natural population analysis. J. Chem. Phys., 1985, 83, 735-746.

Rocha J.C., Martel F., Large neutral amino acids supplementation in phenylketonuric patients. J. Inherit. Metab. Dis., 2009, 32, 472-480.

Shariatinia Z., Shahidi S., A DFT study on the physical adsorption of cyclophosphamide derivatives on the surface of fullerene C_{60} nanocage. J. Mol. Graphics Model., 2014, 52, 71-81.

Sharma S.K., Chiang L.Y., Hamblin M.R., Photodynamic therapy with fullerenes in vivo: reality or a dream? Nanomedicine, 2011, 6, 1813-1825.

Soto-Rojo R., Baldenebro-López J., Flores-Holguín N., Glossman-Mitnik D., Comparison of several protocols for the computational prediction of the maximum absorption wavelength of chrysanthemin. J. Mol. Model., 2014, 20, 2378.

Suliman F.O., Al-Nafai I., Al-Busafi S.N., Synthesis, characterization and DFT calculation of 4-fluorophenyl substituted tris(8-hydroxyquinoline)aluminum(III) complexes. Spectrochim. Acta A, 2014, 118, 66-72.

Sun J., Furness J.W., Zhang Y., Chapter 4 – Density functional theory. Mathematical Physics in Theoretical Chemistry, Developments in Physical & Theoretical Chemistry. Elsevier, 2019.

Tachibana S., Suzuki M., Asano Y., Application of an enzyme chip to the microquantification of l-phenylalanine. Anal. Biochem., 2006, 359, 72-78.

Triesscheijn M., Baas P., Schellens J.H., Stewart F.A., Photodynamic therapy in oncology. Oncologist, 2006, 11, 1034-1044.

van Spronsen F.J., Enns G.M., Future treatment strategies in phenylketonuria. Mol. Genet. Metab., 2010, 99, 90-95.

Wróbel D., Graja A., Photoinduced electron transfer processes in fullerene–organic chromophore systems. Coord. Chem. Rev., 2011, 255, 2555-2577.

Xiao L., Takada H., Maeda K., Haramoto M., Miwa N., Antioxidant effects of water-soluble fullerene derivatives against ultraviolet ray or peroxylipid through their action of scavenging the reactive oxygen species in human skin keratinocytes. Biomed. Pharmacother., 2005, 59, 351-358.

Zhao Y., Truhlar D.G., The M06 suite of density functionals for main group thermochemistry, thermochemical kinetics, noncovalent interactions, excited states, and transition elements: Two new functionals and systematic testing of four M06-class functionals and 12 other functionals. Theor. Chem. Acc., 2007, 120, 215-241.